Robust Microphase Separation Through Chemical Reaction Networks

Franco Blanchini, *Senior Member, IEEE*, Elisa Franco, *Senior Member, IEEE*, Giulia Giordano, *Senior Member, IEEE*, and Dino Osmanović

***Abstract*—The interaction of phase-separating systems with chemical reactions is of great interest in various contexts, from biology to material science. In biology, phase separation is thought to be the driving force behind the formation of biomolecular condensates, i.e., organelles without a membrane that are associated with cellular metabolism, stress response, and development. RNA, proteins, and small molecules participating in the formation of condensates are also involved in a variety of biochemical reactions: how do the chemical reaction dynamics influence the process of phase separation? Here we are interested in finding chemical reactions that can arrest the growth of condensates, generating stable spatial patterns of finite size (microphase separation), in contrast with the otherwise spontaneous (unstable) growth of condensates. We consider a classical continuum model for phase separation coupled to a chemical reaction network (CRN), and we seek conditions for the emergence of stable oscillations of the solution in space. Given reaction dynamics with uncertain rate constants, but known structure, we derive easily computable conditions to assess whether microphase separation is impossible, possible for some parameter values, or robustly guaranteed for all parameter values within given bounds. Our results establish a framework to evaluate which classes of CRNs favor the emergence of condensates with finite size, a question that is broadly relevant to understanding and engineering life.**

***Index Terms*—Chemical reaction networks, phase separation, robustness analysis, stability, uncertain systems.**

Manuscript received 15 March 2023; revised 12 May 2023; accepted 31 May 2023. Date of publication 7 June 2023; date of current version 30 June 2023. The work of Franco Blanchini was supported by the European Union under the NextGenerationEU Grant Uniud-DM737. The work of Elisa Franco and Dino Osmanović was supported in part by the Sloan Foundation under Award G-2021-16831, and in part by the U.S. NSF under CAREER Award 1938194 and FMRG:Bio Award 2134772. The work of Giulia Giordano was supported by the European Union under the ERC INSPIRE Grant 101076926. Recommended by Senior Editor F. Dabbene. *(Corresponding author: Giulia Giordano.)*

Franco Blanchini is with the Department of Mathematics, Computer Science and Physics, University of Udine, 33100 Udine, Italy (e-mail: blanchini@uniud.it).

Elisa Franco and Dino Osmanović are with the Department of Mechanical and Aerospace Engineering, University of California at Los Angeles, Los Angeles, CA 90095 USA (e-mail: efranco@seas.ucla.edu; osmanovic.dino@gmail.com).

Giulia Giordano is with the Department of Industrial Engineering, University of Trento, 38122 Trento, Italy (e-mail: giulia.giordano@unitn.it).

Digital Object Identifier 10.1109/LCSYS.2023.3283934

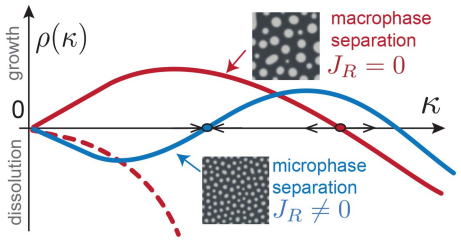

Fig. 1. Dispersion relation curves for phase separating systems. Condensate size grows when the wave number κ decreases. When there is no separation (red, dashed curve), condensates dissolve. In macrophase separation (red, solid curve), typical in the absence of chemical reactions, condensates either grow until they are macroscopically separated (for small κ) or dissolve completely (for large κ), as the intermediate crossing point is an unstable fixed point. In microphase separation (blue curve), which can be induced by chemical dynamics, both large condensates (small κ) and small condensates (large κ) have a negative growth rate, while condensates of intermediate size have a positive growth rate, hence the mid crossing point is a stable fixed point, leading to a prevalent condensate size.

I. Modelling Microphase Separation in the Presence of Chemical Reactions

PHASE separation has emerged as a key area within biological research over the last decade [4]. The physical properties of phase separation are hypothesized to enable living organisms to exercise fine control over their chemical production [22]. Within the non-equilibrium cellular environment, chemical reactions and phase separation combine to produce a new class of physical systems, deemed *active emulsions* [30] or *active droplets* [31]. Beyond biological relevance, these systems have displayed intriguing properties in their own right [23], [26], yielding novel behavior in both spatial organization and dynamical properties. By combining both *conserved* dynamics (phase separation) and *non-conserved* dynamics (chemical reactions), we can think of active emulsions as an extension of classical reaction-diffusion models [3], [19], [20], [21], [24], [25], and bring similar tools to bear on the analysis of their properties. Here we are interested in establishing whether chemical reactions can provide control over phase separating systems by inducing *microphase separation* (MS), *i.e.,* stable patterns of finite size, as opposed to *macrophase separation*, *i.e.,* patterns that expand, or *no phase separation* (Fig. 1).

We model such systems by considering the time evolution of n chemical species, with a vector of concentrations $c(z) = [c_1(z)\, c_2(z)\, \ldots\, c_n(z)] \in \mathbb{R}^n_+$, $z \in \mathbb{R}^{d_s}$. Without loss of

generality, we assume that species 1 phase separates, so it can be in either of two phases, condensed and dispersed, respectively characterized by concentrations c_1^c and c_1^d. The overall dynamics is described by equation:

$$\frac{\mathrm{d}c(z,t)}{\mathrm{d}t} = \mathbf{I}(c(z,t)) + \mathbf{R}(c(z,t)), \tag{1}$$

where the term $\mathbf{I}(c(z,t)) = \nabla \cdot (\mathfrak{D}\nabla \frac{\delta F(c(z,t))}{\delta c(z,t)})$ describes conserved spatial dynamics, under the Cahn-Hilliard [12] energy functional $F(c(z,t)) = \int \{\nu(c_1(z) - c_1^c)^2(c_1(z) - c_1^d)^2 + \gamma^2|\nabla c_1(z)|^2 + \frac{1}{2}c^\top \epsilon c\}dz$, where $\gamma > 0$ is a length scale, $\epsilon \in \mathbb{R}^{n\times n}$ is a matrix of constant attraction/repulsion parameters, and ν is an energy scale. See also [27] and [14], [29] for similar approaches combining the Cahn-Hilliard model for phase separation and chemical dynamics. We infer the corresponding time evolution via "model B" dynamics [18]. We assume that every species has the same homogeneous diffusion coefficient and molecular mass, hence the diffusion matrix is $\mathfrak{D} = dI$, where $d > 0$ is a common diffusion constant. The term $\mathbf{R}(c(z,t))$ describes the reaction fluxes generated by a set of chemical reactions, assuming the existence of a free energy source that maintains the rates at which the reactions proceed [26].

Full analysis of (1) is usually rather complex, however we can obtain information about the properties of the solution by linearization (i.e., by treating each Fourier mode of the system as independent and observing whether that mode is unstable to infinitesimal perturbations), which can give tractable results on the effects of chemistry on phase separation. Linearization is a canonical method of treating reaction-diffusion like problems; [16, Sec. III] and [29, SI] provide details about linearization in a combined phase separation/reaction model. We perform a linear stability analysis of model (1) near the fixed point of the chemical dynamics $\mathbf{R}(c_s) = 0$: $c(z,t) = c_s + w\exp(i\kappa z + \rho(\kappa)t)$, where w is small: $w^2 \approx 0$. The linearization around c_s involves the Jacobian matrices $J_I(\kappa) = \nabla_{c(z)}\mathbf{I}(c(z,t))|_{c=c_s}$ of the conserved spatial dynamics and $J_R = \nabla_{c(z)}\mathbf{R}(c(z,t))|_{c=c_s}$ of the chemical reaction dynamics. We assume that the phase-separating species is the first one, so that $J_I(\kappa)$ has the symmetric structure:

$$J_I(\kappa) = \begin{bmatrix} \mu|\kappa|^2 - \gamma^2|\kappa|^4 & -d|\kappa|^2\epsilon_{12} & \dots & -d|\kappa|^2\epsilon_{1n} \\ -d|\kappa|^2\epsilon_{12} & -d|\kappa|^2 & \dots & -d|\kappa|^2\epsilon_{2n} \\ \vdots & \vdots & \ddots & \vdots \\ -d|\kappa|^2\epsilon_{1n} & -d|\kappa|^2\epsilon_{2n} & \dots & -d|\kappa|^2 \end{bmatrix}, \tag{2}$$

where ϵ_{ij} represent spatial attraction/repulsion among species, and $\mu > 0$ depends on d, c_1^c, c_1^d and c_s. We thus obtain the relationship

$$\rho(\kappa)w = [J_I(\kappa) + J_R]w, \tag{3}$$

where the spectral abscissa $\rho(\kappa)$ of $(J_I(\kappa) + J_R)$ characterizes the dynamics of spatially oscillatory behaviors. The *dispersion relation* curve $\rho(\kappa)$ depends on the wave number κ: the growth rate of a spatial wave depends on its wave number. For more information about dispersion curves, see e.g., [11], [16].

Linearization allows us to make quantitative predictions about the behavior of a given system without computing the full solution to (1). We can use linearization to discriminate between systems that undergo *microphase separation* (MS), *macrophase separation* or *no phase separation*. As previously mentioned, MS corresponds to finite size patterns that do not change over time: as illustrated in Fig. 1, this happens when $\rho(\kappa) < 0$ for small κ, $\rho(\kappa) > 0$ for intermediate κ, and $\rho(\kappa) < 0$ for large κ. In MS, spatial compartmentalization occurs with a particular length scale, enabling precise control of droplets that can operate like microreactors with "life-like" properties [30].

The design space of such a problem is large, in that we have many possible chemical reaction networks (CRNs) that can couple to phase separating systems. To assess the likelihood of MS and identify interesting candidate CRNs for experimental realization, in previous work we computationally explored the parameters and chemical reaction networks that lead to matrices $J_I(\kappa)$ and J_R in (3) [27]. The probability that $\rho(\kappa)$ has three roots was evaluated when generating either random J_R matrices or random CRNs [28].

Here we consider the problem of inducing MS via chemical reactions through a control-theoretic approach. Given a CRN structure, whose rate parameters are unknown but bounded in a known range, we rely on parametric robustness approaches [5] and vertex results [9], [10], [17] to provide conditions ensuring that MS is: *impossible*; *possible for some parameter values*; or *robustly guaranteed for all parameter values in the range*.

We achieve these conditions by converting the original problem, formulated in terms of the spectral abscissa of an uncertain matrix and thus challenging to handle, into a problem formulated in terms of the robust analysis of the determinant of an uncertain matrix, much simpler to deal with.

II. Microphase Separation: A Spectral Problem

To characterize the dispersion relation (3), we study the spectrum of matrix $J(\kappa) = J_I(\kappa) + J_R$. Given (2), by collecting the terms in $|\kappa|^2$ and $|\kappa|^4$ we can write $J_I(\kappa) = J_2|\kappa|^2 + J_4|\kappa|^4$ and $J(\kappa)$ becomes:

$$J(\kappa) = J_R + J_2|\kappa|^2 + J_4|\kappa|^4. \tag{4}$$

Without restriction, we assume that J_R can be rewritten according to the *BDC decomposition* introduced in [6], [7], [17]; this is possible for the Jacobian of any generic CRN.

Assumption 1: The Jacobian J_R can be decomposed as $J_R = B\Delta C$, where $\Delta = \mathrm{diag}\{\Delta_1, \Delta_2, \dots, \Delta_m\}$ has positive diagonal entries representing the uncertain parameters (the nonzero partial derivatives of the CRN system), while matrices $B \in \mathbb{Z}^{n\times m}$ and $C \in \mathbb{Z}^{m\times n}$ represent the known structure of the given CRN. The unknown parameters Δ_j are bounded as

$$\Delta \in \mathcal{D} = \{\Delta : 0 < \Delta_j^- \le \Delta_j \le \Delta_j^+\}, \tag{5}$$

for given lower bounds Δ_j^- and upper bounds Δ_j^+.

We restrict our analysis to CRNs with one conservation law.

Assumption 2: For all $\Delta \in \mathcal{D}$, matrix $J_R = B\Delta C$ is singular and has $n-1$ eigenvalues with negative real part. Also, there exists a nonnegative vector $v^\top \ge 0$ such that $v^\top B = 0$, representing a conservation law: since $v^\top B\Delta C = 0$, $v^\top$ is a left eigenvector of J_R associated with the eigenvalue at 0.

Assumption 2 entails that matrix J_R is marginally stable. Its stability can be assessed through several existing techniques tailored to CRNs, proposed for instance in [1], [6], [8], [15].

We also introduce suitable assumptions on the symmetric matrix $J_I(\kappa) = J_2|\kappa|^2 + J_4|\kappa|^4$.

Assumption 3: The symmetric matrix J_2 is indefinite, the symmetric matrix J_4 is negative semi-definite, and there exists $\bar{\kappa}$ such that $J_I(\bar{\kappa}) = J_2|\bar{\kappa}|^2 + J_4|\bar{\kappa}|^4$ is negative definite.

The Jacobian matrix $J(\kappa) = J_R + J_2|\kappa|^2 + J_4|\kappa|^4$ in (4) has eigenvalues $\lambda_i(\Delta, \kappa)$, $i = 1, \ldots, n$, and its spectral abscissa (namely, the maximum real part $\Re$ of its eigenvalues) is

$$\rho(\Delta, \kappa) = \max_i \{\Re(\lambda_i(\Delta, \kappa)\}.$$

The eigenvalues of $J_R = B\Delta C$ are $\lambda_i(\Delta, 0)$, $i = 1, \ldots, n$.

Assumption 4: The eigenvalue of matrix $J_R = B\Delta C$ associated with the conservation law is $\lambda_1(\Delta, 0) = 0$.

Definition 1: A continuous function $f(\kappa)$ has a positive sign change if $f(\kappa_1) < 0 < f(\kappa_2)$ for some $\kappa_1 < \kappa_2$, while it has a negative sign change if $f(\kappa_1) > 0 > f(\kappa_2)$. Moreover, function $f(\kappa)$ is initially positive (respectively, negative) if there exists an open right neighborhood of 0, $(0, \hat{\kappa})$, in which the function is positive (respectively, negative).

We can now define the (robust) microphase separation property that is the subject of our analysis.

Definition 2 (Occurrence of Microphase Separation): System (1) exhibits microphase separation (MS) if, for a given $\Delta \in \mathcal{D}$, $\rho(\Delta, \kappa)$ is initially negative (i.e., there exists $\hat{\kappa}$ such that $\rho(\Delta, \kappa) < 0$ for all $\kappa \in (0, \hat{\kappa})$), then has a positive sign change and finally a negative sign change (i.e., $\rho(\Delta, \kappa_1) > 0$ and $\rho(\Delta, \kappa_2) < 0$ for some $0 < \hat{\kappa} < \kappa_1 < \kappa_2$). System (1) exhibits robust MS if this condition holds for all $\Delta \in \mathcal{D}$.

The MS condition in Definition 2 describes a qualitative behavior of $\rho(\Delta, \kappa)$ consistent with the blue curve in Fig. 1: the size of condensates shrinks for small κ, grows for intermediate values of κ, shrinks again for large κ. For known parameters, the condition can be tested by directly computing the eigenvalue curves [27]. Departing from this approach, our analysis aims to develop efficient methods to tackle the case of *uncertain* CRN parameters: given a range of possible parameter values, by taking advantage of the *BDC* decomposition of the Jacobian of the chemical reaction dynamics, we check whether the condition can or cannot hold for some parameters in the range, and whether it holds *robustly* for all parameters in the range.

III. Robust Determinant Conditions for Microphase Separation

We obtain (robust) conditions for MS by mapping the dispersion relation problem, involving the spectral abscissa $\rho(\Delta, \kappa)$, to a determinant problem. To this aim, given uncertain CRN parameters Δ, whose values are bounded in the set $\mathcal{D}$ as in (5), we consider the functions

$$\Psi^-(\kappa) = \min_{\Delta \in \mathcal{D}} \det[-(B\Delta C + |\kappa|^2 J_2 + |\kappa|^4 J_4)], \quad (6)$$

$$\Psi^+(\kappa) = \max_{\Delta \in \mathcal{D}} \det[-(B\Delta C + |\kappa|^2 J_2 + |\kappa|^4 J_4)], \quad (7)$$

which can be easily computed, as we will show in Section III-B. In view of their definition, $\Psi^-(\kappa) \leq \Psi^+(\kappa)$. Moreover, $\Psi^-(0) = \Psi^+(0) = 0$, because, in view of Assumption 2, the determinants in (6) and (7) are 0 for $\kappa = 0$. Both functions grow to infinity as $\kappa \to +\infty$, as shown after Lemma 1.

Studying functions $\Psi^-(\kappa)$ and $\Psi^+(\kappa)$ allows us to provide:

- a crucial necessary condition for MS: Ψ^+ needs to be initially positive (Theorem 1);
- a sufficient condition ensuring MS for some values of the parameters (which we can determine): *either* Ψ^- *or* Ψ^+ is initially positive and has a negative sign change (Theorem 2);
- a sufficient condition ensuring *robust* MS for all admissible parameters: *both* Ψ^- and Ψ^+ are initially positive and have a negative sign change (Theorem 3).

The technical challenge lies in relating the spectral abscissa $\rho(\Delta, \kappa)$ to the curves Ψ^- and Ψ^+. The difficulty arises from the fact that, while a negative value of the determinant $\det[-(B\Delta C + |\kappa|^2 J_2 + |\kappa|^4 J_4)]$ implies positivity of the spectral abscissa $\rho(\Delta, \kappa)$, the opposite unfortunately is not true: the determinant may well be positive even when $\rho(\Delta, \kappa) > 0$.

We begin by considering the case in which only the chemical reaction parameters are subject to uncertainty, which affects the entries of J_R.

Theorem 1 (Necessary Condition): If system (1) exhibits microphase separation for some $\Delta \in \mathcal{D}$, then Ψ^+ is initially positive.

Proof: Since $\rho(\Delta, \kappa) < 0$ necessarily requires that $\det[-(B\Delta C + |\kappa|^2 J_2 + |\kappa|^4 J_4)] > 0$, then the maximum Ψ^+ must be initially positive when $\rho(\Delta, \kappa)$ is initially negative, as required by Definition 2. ■

In Fig. 2A we illustrate a case in which Ψ^+ is not initially positive, hence MS is not possible; conversely, in Fig. 2B, Ψ^+ is initially positive.

We now state the other main results, whose proof requires some technical lemmas and is thus reported in Section III-A.

Theorem 2 (Sufficient Condition): System (1) exhibits microphase separation for some $\Delta \in \mathcal{D}$ if either Ψ^- or Ψ^+ is initially positive and has a negative sign change.

Actual parameter values for which MS does occur can be found following the procedure described in Section III-B.

In Figs. 2B and 2C, we illustrate the case in which MS is possible for some $\Delta \in \mathcal{D}$.

Theorem 3 (Robust Sufficient Condition): System (1) exhibits microphase separation for all $\Delta \in \mathcal{D}$ if Ψ^- is initially positive (and hence Ψ^+ is initially positive too) and Ψ^+ has a negative sign change (and hence Ψ^- has it too).

In Fig. 2D, we illustrate the case in which MS is robustly guaranteed for all $\Delta \in \mathcal{D}$.

Finally, we briefly touch upon the case in which uncertainty affects the parameters of both spatial dynamics (i.e., the entries of J_I) and chemical dynamics (i.e., the entries of J_R).

Corollary 1: Assume that J_2 and J_4 are diagonal matrices, whose diagonal entries are uncertain parameters bounded in intervals. Then, redefining the functions as $\Psi^-(\kappa) = \min_{\Delta, J_2, J_4} \det[-(B\Delta C + |\kappa|^2 J_2 + |\kappa|^4 J_4)]$ and $\Psi^+(\kappa) = \max_{\Delta, J_2, J_4} \det[-(B\Delta C + |\kappa|^2 J_2 + |\kappa|^4 J_4)]$, all the previous results still hold true.

A. Proofs of the Main Results

We begin with two technical lemmas. The first states that, for large enough κ, we have Hurwitz stability.

Lemma 1: For any given Δ, $\lim_{\kappa \to +\infty} \rho(\Delta, \kappa) = -\infty$.

Proof: Recall that J_4 is negative semi-definite and take $\kappa \geq \bar{\kappa}$, with $\bar{\kappa}$ defined in Assumption 3. The Lyapunov inequality

$$\left(J_R + J_2|\kappa|^2 + J_4|\kappa|^4\right)^\top + \left(J_R + J_2|\kappa|^2 + J_4|\kappa|^4\right)$$
$$= (B\Delta C)^\top + B\Delta C + 2J_2|\kappa|^2 + 2J_4|\kappa|^4$$

$$\leq (B\Delta C)^\top + B\Delta C + 2J_2|\kappa|^2 + 2J_4|\kappa|^2|\bar{\kappa}|^2$$
$$= |\kappa|^2\left[\frac{(B\Delta C)^\top + B\Delta C}{|\kappa|^2} + 2(J_2 + J_4|\bar{\kappa}|^2)\right] < 0 \qquad (8)$$

holds for κ large, because $(J_2 + J_4|\bar{\kappa}|^2)$ is negative definite and the fraction converges to 0. This implies Hurwitz stability for κ large enough. To prove that $\lim_{\kappa\to\infty}\rho(\Delta,\kappa) = -\infty$, denote $K = B\Delta C + \kappa I$ and repeat the computation for the perturbed matrix $J_\kappa = (\kappa I + J_R + J_2|\kappa|^2 + J_4|\kappa|^4)$ to get

$$J_\kappa^\top + J_\kappa \leq |\kappa|^2\left[\frac{K^\top + K}{|\kappa|^2} + 2(J_2 + J_4|\bar{\kappa}|^2)\right] < 0 \qquad (9)$$

for κ large, hence J_κ is Hurwitz. The spectral abscissa of $(J_R + J_2|\kappa|^2 + J_4|\kappa|^4)$ is thus less than $-\kappa$, for κ large. ■

Since the determinant of the negative of a matrix of size n is $(-1)^n$ times the product of the matrix eigenvalues, $\lim_{\kappa\to+\infty}\rho(\Delta,\kappa) = -\infty$ implies that $\lim_{\kappa\to+\infty}\Psi^-(\kappa) = \lim_{\kappa\to+\infty}\Psi^+(\kappa) = +\infty$.

Remark 1: If we take bounds $\Delta_i^- > 0$ and $\Delta_i^+ < \infty$, by compactness the limit in Lemma 1 is uniform in $\Delta \in \mathcal{D}$.

Due to Lemma 1, if $\rho(\Delta,\kappa)$ has a positive sign change, then it needs to have a subsequent negative sign change.

Lemma 2: Under Assumption 2, if for some Δ we have that $\det[-(B\Delta C + |\kappa|^2 J_2 + |\kappa|^4 J_4)]$ is initially positive, as a function of κ, then there exists $\tilde{\kappa} > 0$ such that $\rho(\Delta,\kappa) < 0$ for $0 < \kappa \leq \tilde{\kappa}$.

Proof: Consider the characteristic polynomial

$$p(s,\kappa,\Delta) = \det[sI - (B\Delta C + |\kappa|^2 J_2 + |\kappa|^4 J_4)]. \qquad (10)$$

For $\kappa = 0$, $\lambda_1 = 0$ is an isolated root of the characteristic polynomial $p(s,0,\Delta)$, while all the other roots λ_i, $i > 1$, have negative real parts. In view of the continuity of the eigenvalues with respect to κ, for a small, positive κ the roots λ_i, $i > 1$, still have negative real part. Hence, the spectral abscissa is given by the dominant real eigenvalue λ_1 and we show that, for a small, positive κ, λ_1 becomes negative, hence $\rho(\Delta,\kappa) < 0$. We can write the characteristic polynomial as

$$p(s,\kappa,\Delta) = s^n + p_{n-1}(\kappa,\Delta)s^{n-1} + \cdots + p_1(\kappa,\Delta)s + p_0(\kappa,\Delta).$$

For $\kappa = 0$, the constant term $p_0(0,\Delta) = 0$, due to the zero root, while $p_j(0,\Delta) > 0$ for $j > 0$, since all other roots have negative real part in view of Assumption 2. Hence the derivative of p computed at $s = 0$, assuming s real, is positive: $\frac{d}{ds}p(s,\kappa,\Delta)|_{s=0} = p_1(\kappa,\Delta) > 0$. For a small, positive κ in a neighborhood of 0, the polynomial $p(s,\kappa,\Delta)$ becomes positive and, since it is locally increasing in κ, the root λ_1, which is initially 0, moves to the left and becomes negative. ■

We are now ready to prove Theorem 2.

Proof: If Ψ^- is initially positive, then for all Δ, $p(s,\kappa,\Delta)$ defined in (10) is initially positive. Lemma 2 ensures that $\rho(\Delta,\kappa) < 0$ in a right neighborhood of zero, for all Δ. On the other hand, Ψ^- becomes negative for some larger κ, meaning that for some Δ^*, $\rho(\Delta^*,\kappa) > 0$, so $\rho(\Delta^*,\kappa)$ has a positive sign change. Then, ρ will have a negative sign change $\rho(\Delta^*,\kappa) < 0$ for κ large in view of Lemma 1.

If Ψ^+ is initially positive, then for some Δ^*, $p(s,\kappa,\Delta^*)$ is initially positive. In view of Lemma 2, $\rho(\Delta^*,\kappa) < 0$ in a right neighborhood of zero, for all Δ. On the other hand, Ψ^+ becomes negative for some larger κ, meaning that $\rho(\Delta,\kappa) > 0$ for all Δ. Then $\rho(\Delta^*,\kappa) < 0$ has a positive sign change, and eventually will have a negative sign change $\rho(\Delta^*,\kappa) < 0$ for κ large, again, in view of Lemma 1. ■

Finally, we prove Theorem 3.

Proof: If Ψ^- is initially positive, then $\rho(\Delta,\kappa)$ is initially negative for all Δ. If Ψ^+ has a negative sign change, then $\rho(\Delta,\kappa)$ becomes positive for all Δ (before becoming eventually negative). ■

Remark 2: If $\rho(\Delta,\kappa)$ becomes positive, we cannot discriminate whether the ensuing transition to instability is due to the appearance of real or complex eigenvalues (unless J_R is Metzler, as in the case of networks of mono-molecular reactions, and J_I is diagonal, so that the dominant eigenvalue is real). We believe that a supplementary analysis can be performed resorting to value-set techniques [5] or to second additive compound matrices [2] so as to possibly rule out imaginary eigenvalues.

Corollary 1 can be proven by repeating the same arguments as above, since the determinant is a multilinear function of all the considered parameters if matrices J_2 and J_4 are diagonal.

B. Computing Ψ^- and Ψ^+ and Checking Criteria

Computing Ψ^- and Ψ^+ is simple, since they are respectively the minimum and the maximum of 2^m polynomials.

Proposition 1: Given the set $\mathcal{D}$ in (5), let $\hat{\mathcal{D}}$ be the set of all its vertices: $\hat{\mathcal{D}} = \{\Delta{:}\Delta_j \in \{\Delta_j^-, \Delta_j^+\}\}$. Then, the functions Ψ^- and Ψ^+, respectively defined in (6) and (7), can be computed as

$$\Psi^-(\kappa) = \min_i p_i(\kappa), \qquad \Psi^+(\kappa) = \max_i p_i(\kappa), \qquad (11)$$

where $p_i(\kappa) = \det[-(B\Delta^{(i)}C + |\kappa|^2 J_2 + |\kappa|^4 J_4)]$ with $\Delta^{(i)} \in \hat{\mathcal{D}}$, $i = 1, 2, \ldots, 2^m$.

The curves Ψ^- and Ψ^+ are thus piecewise polynomials: there exists a finite set of values $\kappa_1, \kappa_2, \ldots, \kappa_M$ for which Ψ^- (analogously, Ψ^+) is a polynomial in each interval $[\kappa_h, \kappa_{h+1}]$. Hence, Ψ^- and Ψ^+ are piecewise differentiable.

Proof: For any value of κ, the maximum and minimum in (6) and (7) are achieved on the vertices $\hat{\mathcal{D}}$ of the hyper-rectangle $\mathcal{D}$, because the determinants are multilinear functions of the uncertain parameters Δ_i and any multilinear function defined on a hyper-rectangle achieves both its minimum and its maximum value on a vertex [5], [9], [10].

The fact that the curves Ψ^- and Ψ^+ are piecewise polynomials follows from the fact that two different polynomials of order N can intersect in at most N points. ■

It can be immediately seen that Proposition 1 allows us to check the conditions of Theorems 1, 2 and 3 as follows.

Proposition 2: The following equivalences hold.

- Ψ^- is initially positive iff all the polynomials $p_i(\kappa)$ are initially positive.
- Ψ^+ is initially positive iff at least one of the polynomials $p_i(\kappa)$ is initially positive.
- Ψ^- takes negative values iff at least one of $p_i(\kappa)$ does.
- Ψ^+ takes negative values iff all $p_i(\kappa)$ do.

Remarkably, checking the conditions for MS requires the analysis of a finite number of polynomials. When the sufficient conditions of Theorem 2 are met, and thus the considered CRN structure can give rise to MS *provided that the parameters are suitably chosen*, the following algorithm allows us to identify values that do ensure MS.

Algorithm 1: To find parameter values ensuring MS:

- If Ψ^- is initially positive and has a negative sign change, find κ^* for which $\Psi^-(\kappa^*) < 0$. Then, the vertex polynomial p_h such that $p_h(\kappa^*) = \Psi^-(\kappa^*) < 0$ is associated with vertex parameters $\Delta^*_{sep} \in \hat{\mathcal{D}}$ ensuring MS.
- If Ψ^+ is initially positive and has a negative sign change, find $\tilde{\kappa}$ such that, for $0 < \kappa \leq \tilde{\kappa}$, the vertex polynomial $p_h(\kappa) = \Psi^+(\kappa) > 0$. Then, p_h is associated with vertex parameters $\tilde{\Delta}_{sep} \in \hat{\mathcal{D}}$ ensuring MS.

Remark 3: The algorithm finds a vertex at which MS is verified. Then, a region where MS is robustly verified can be easily determined. Assume, e.g., that we are in the first case and the identified vertex has $\Delta_i = \Delta_i^-$. Consider the reduced region $[\Delta_i^-, \Delta_i^- + \lambda(\Delta_i^+ - \Delta_i^-)]$, with $0 < \lambda < 1$. By iterating over decreasing λ, we may find that also Ψ^+ has a sign change: $\Psi^+(\kappa^*) < 0$. Then, MS is robustly guaranteed within the whole reduced region according to Theorem 3.

IV. Testing Microphase Separation in the Presence of Chemical Reactions

We provide here a collection of examples where we apply our proposed criteria to test robust microphase separation in the presence of different chemical reaction network structures. In all the considered examples, we assume $|\kappa|^2 J_2 + |\kappa|^4 J_4 = \text{diag}\big[\mu|\kappa|^2 - \gamma^2|\kappa|^4 \quad -d|\kappa|^2 \quad -d|\kappa|^2 \quad \dots \quad -d|\kappa|^2\big]$, so that the separating species is the first one (C_1), and we take $\mu = 1$, $d = 1$ and $\gamma^2 = 0.03$.

Example 1: Consider the CRN $C_1 + C_3 \rightharpoonup C_2 + C_4$, $C_2 \rightharpoonup C_1$, $C_4 \rightharpoonup \emptyset$, $\emptyset \rightharpoonup C_3$. The CRN system is formed by equations $\dot{c}_1 = -g_{13}(c_1, c_3) + g_2(c_2) = -\dot{c}_2$, $\dot{c}_3 = -g_{13}(c_1, c_3) + c_0$, $\dot{c}_4 = +g_{13}(c_1, c_3) - g_4(c_4)$, corresponding to the *BDC*-decomposable Jacobian matrix $J = B\Delta C$, with

$$B = \begin{bmatrix} -1 & 1 & -1 & 0 \\ 1 & -1 & 1 & 0 \\ -1 & 0 & -1 & 0 \\ 1 & 0 & 1 & -1 \end{bmatrix}, \quad C = \begin{bmatrix} 1 & 0 & 0 & 0 \\ 0 & 1 & 0 & 0 \\ 0 & 0 & 1 & 0 \\ 0 & 0 & 0 & 1 \end{bmatrix},$$

$\Delta = \text{diag}\Big[\frac{\partial g_{13}}{\partial c_1} \quad \frac{\partial g_2}{\partial c_2} \quad \frac{\partial g_{13}}{\partial c_3} \quad \frac{\partial g_4}{\partial c_4}\Big]$. With bounds $\Delta_i^+ = 0.5$ and $\Delta_i^- = 0.3$ for all i, functions Ψ^- and Ψ^+ are visualised in Fig. 2A. The necessary condition in Theorem 1 is violated, because Ψ^+ is initially negative, hence MS is never possible for $\Delta \in \mathcal{D}$. Fig. 2A1 illustrates the lack of MS on the full nonlinear simulation of a 2D system with $g_{13} = 0.856c_1c_2$, $g_2 = 0.84c_2$, $c_0 = 0.59$, $g_4 = 0.8c_4$.

Example 2: Consider the CRN $C_1 \rightharpoonup C_2 \rightharpoonup C_3 \rightharpoonup C_1$ corresponding to equations $\dot{c}_1 = -g_1(c_1) + g_3(c_3)$, $\dot{c}_2 = -g_2(c_2) + g_1(c_1)$, $\dot{c}_3 = -g_3(c_3) + g_2(c_2)$, with Jacobian $J = B\Delta C$,

$$B = \begin{bmatrix} -1 & 0 & 1 \\ 1 & -1 & 0 \\ 0 & 1 & -1 \end{bmatrix}, \; C = \begin{bmatrix} 1 & 0 & 0 \\ 0 & 1 & 0 \\ 0 & 0 & 1 \end{bmatrix},$$
$$\Delta = \text{diag}\Big[\frac{\partial g_1}{\partial c_1} \; \frac{\partial g_2}{\partial c_2} \; \frac{\partial g_3}{\partial c_3}\Big].$$

Taking $\Delta_i^- = 2$ and $\Delta_i^+ = 5$ for all i, Fig. 2B shows that MS is possible, because the condition in Theorem 2 is satisfied: Ψ^+ is initially positive and has a negative sign change. A parameter choice ensuring MS is $\tilde{\Delta}_{sep} = \begin{bmatrix} 5 & 2 & 2 \end{bmatrix}$, computed following Algorithm 1. Fig. 2B1 shows MS emergence

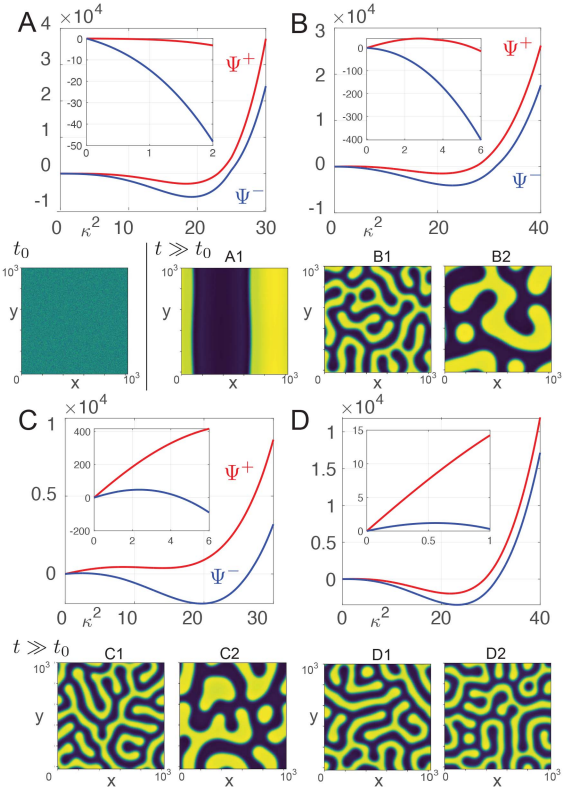

Fig. 2. Ψ^- (blue) and Ψ^+ (red) for the different examples we considered. In Example 1 (panel A), Ψ^+ is initially negative, thus violating the necessary condition in Theorem 1: MS never occurs for $\Delta \in \mathcal{D}$. In Example 2 (panel B), Ψ^+ is initially positive and has a negative sign change: MS occurs for some $\Delta \in \mathcal{D}$. In Example 3 (panel C), Ψ^- is initially positive and has a negative sign change: MS occurs for some $\Delta \in \mathcal{D}$. In Example 4 (panel D), Ψ^- (hence Ψ^+) is initially positive and then Ψ^+ (hence Ψ^-) changes sign: MS occurs robustly for all $\Delta \in \mathcal{D}$. Bottom row panels (A1, B1, B2, C1, C2, D1, D2): full nonlinear simulations of the examples considered, starting from the same initial conditions (t_0); occurrence of MS matches the expectation of our linear analysis. Simulation parameters are in the main text. Full simulations can be downloaded at `https://github.com/osmanovicdino/CRNData`.

is possible in the full nonlinear system for $g_1 = 0.57c_1$, $g_2 = 0.27c_2$ and $g_3 = 0.98c_3$, which correspond to an initially negative dispersion relation. Picking a different parameter set, which violates the conditions of Theorem 2, does not lead to MS as shown in Fig. 2B2, where $g_1 = 0.58c_1$, $g_2 = 0.13c_2$ and $g_3 = 0.78c_3$. Patterns coarsen slowly; at $t \to \infty$ they are expected to match those in Fig. 2A1.

Example 3: Consider the CRN $C_1 \rightleftharpoons C_2$, $C_1 + C_2 \rightleftharpoons C_3$ and the corresponding system $\dot{c}_1 = -g_{12}(c_1, c_2) - g_1(c_1) + g_2(c_2) + g_3(c_3)$, $\dot{c}_2 = -g_{12}(c_1, c_2) + g_1(c_1) - g_2(c_2) + g_3(c_3)$, $\dot{c}_3 = g_{12}(c_1, c_2) - g_3(c_3)$, which has Jacobian $J = B\Delta C$ with

$$B = \begin{bmatrix} -1 & 1 & -1 & -1 & 1 \\ 1 & -1 & -1 & -1 & 1 \\ 0 & 0 & 1 & 1 & -1 \end{bmatrix}, \quad C = \begin{bmatrix} 1 & 0 & 1 & 0 & 0 \\ 0 & 1 & 0 & 1 & 0 \\ 0 & 0 & 0 & 0 & 1 \end{bmatrix}^\top,$$

$\Delta = \text{diag}\Big[\frac{\partial g_1}{\partial c_1} \quad \frac{\partial g_2}{\partial c_2} \quad \frac{\partial g_{12}}{\partial c_1} \quad \frac{\partial g_{12}}{\partial c_2} \quad \frac{\partial g_3}{\partial c_3}\Big]$. When $\Delta_i^- = 3$ and $\Delta_i^+ = 5$ for all i, as shown in Fig. 2C, MS is possible, because the condition in Theorem 2 is satisfied: Ψ^- is initially positive and has a negative sign change. A parameter choice ensuring MS is $\Delta^*_{sep} = \begin{bmatrix} 3 & 5 & 3 & 3 & 5 \end{bmatrix}$, computed following Algorithm 1. Figs. 2C1 and C2 show nonlinear simulations in which the system respectively does

($g_1 = 0.27c_1$, $g_2 = 0.92c_2$, $g_{12} = 0.14c_1c_2$, $g_3 = 0.77c_3$) or does not ($g_1 = 0.54c_1$, $g_2 = 0.5c_2$, $g_{12} = 0.72c_1c_2$, $g_3 = 0.77c_3$) exhibit MS, as expected from our linear analysis.

Example 4: Consider the CRN $C_1 \rightleftharpoons C_2 \rightleftharpoons C_3$, corresponding to system $\dot{c}_1 = -g_1(c_1)+g_{2,1}(c_2)$, $\dot{c}_2 = -g_{2,1}(c_2)+g_1(c_1)-g_{2,2}(c_2)+g_3(c_3)$, $\dot{c}_3 = -g_3(c_3)+g_{2,2}(c_2)$, which has Jacobian $J = B\Delta C$

$$B = \begin{bmatrix} -1 & 1 & 0 & 0 \\ 1 & -1 & -1 & 1 \\ 0 & 0 & 1 & -1 \end{bmatrix}, \quad C = \begin{bmatrix} 1 & 0 & 0 & 0 \\ 0 & 1 & 1 & 0 \\ 0 & 0 & 0 & 1 \end{bmatrix}^\top,$$

$\Delta = \text{diag}\left[\frac{\partial g_1}{\partial c_1} \quad \frac{\partial g_{2,1}}{\partial c_2} \quad \frac{\partial g_{2,2}}{\partial c_2} \quad \frac{\partial g_3}{\partial c_3}\right]$. Taking $\Delta_i^- = 1$ and $\Delta_i^+ = 2$ for all i, Fig. 2D shows that MS occurs robustly, for all choices of Δ within the bounds, because the condition in Theorem 3 is satisfied: both Ψ^- and Ψ^+ are initially positive and have a negative sign change. Figs. 2D1 and D2 show example nonlinear simulations with two arbitrary parameter sets in which the system always exhibits MS ($g_1 = 0.65c_1$, $g_{2,1} = 0.09c_2$, $g_{2,} = 0.69c_2$, $g_3 = 0.37c_3$ for D1 and $g_1 = 0.74c_1$, $g_{2,1} = 0.03c_2$, $g_{2,2} = 0.22c_2$, $g_3 = 0.66c_3$ for D2) consistent with the expectation from the linear analysis.

V. Concluding Discussion

Recent work [13], [14], [23] has extended the reaction-diffusion framework to account for more complex models of diffusive dynamics, such as usage of the Cahn-Hilliard functional to model the conserved dynamics corresponding to phase separation. While many studies have focused on traditional reaction-diffusion systems [3], [19], [20], [21], [24], [25], we are only beginning to explore phase separating systems subject to chemical reactions, which can lead to intriguing structural and dynamical properties [31].

We have considered the problem of predicting the emergence of microphase separation (MS) in a continuum model that couples phase separation and chemical reactions: spatial dynamics affect how species arrange in space while keeping their total concentration constant; chemical reaction dynamics determine how the species locally inter-convert, thus changing the total amounts of individual components. MS is associated with the occurrence of stable spatial oscillations with regions of high density of material, known as condensates. For uncertain chemical reaction parameters bounded in a known interval, we have provided easy-to-compute conditions to check whether MS can be ruled out, or can arise for some parameters in the interval, or does robustly arise for all parameters in the interval. Our approach offers useful tools and insights for the experimental design of robust phase-separating systems in synthetic biology or material science.

References

[1] M. A. Al-Radhawi and D. Angeli, "New approach to the stability of chemical reaction networks: Piecewise linear in rates Lyapunov functions," *IEEE Trans. Autom. Control*, vol. 61, no. 1, pp. 76–89, Jan. 2016.

[2] D. Angeli, M. Banaji, and C. Pantea, "Combinatorial approaches to Hopf bifurcations in systems of interacting elements," *Commun. Math. Sci.*, vol. 12, no. 6, pp. 1101–1133, 2014.

[3] M. Arcak, "Certifying spatially uniform behavior in reaction-diffusion PDE and compartmental ODE systems," *Automatica*, vol. 47, no. 6, pp. 1219–1229, 2011.

[4] S. F. Banani, H. O. Lee, A. A. Hyman, and M. K. Rosen, "Biomolecular condensates: Organizers of cellular biochemistry," *Nat. Rev. Mol. Cell Biol.*, vol. 18, pp. 285–298, Feb. 2017.

[5] B. R. Barmish, *New Tools for Robustness of Linear Systems*. New York, NY, USA: Macmillan, 1994.

[6] F. Blanchini and G. Giordano, "Piecewise-linear Lyapunov functions for structural stability of biochemical networks," *Automatica*, vol. 50, no. 10, pp. 2482–2493, 2014.

[7] F. Blanchini and G. Giordano, "Structural analysis in biology: A control theoretic approach," *Automatica*, vol. 126, Apr. 2021, Art. no. 109376.

[8] F. Blanchini, G. Chesi, P. Colaneri, and G. Giordano, "Checking structural stability of *BDC*-decomposable systems via convex optimisation," *IEEE Control Syst. Lett.*, vol. 4, pp. 205–210, 2020.

[9] F. Blanchini, P. Colaneri, G. Giordano, and I. Zorzan, "Predicting adaptation for uncertain systems with robust real plots," in *Proc. 59th IEEE Conf. Decis. Control (CDC)*, 2020, pp. 5861–5866.

[10] F. Blanchini, P. Colaneri, G. Giordano, and I. Zorzan, "Vertex results for the robust analysis of uncertain biochemical systems," *J. Math. Biol.*, vol. 85, p. 35, Sep. 2022.

[11] C. A. Brackley, B. Liebchen, D. Michieletto, F. Mouvet, P. R. Cook, and D. Marenduzzo, "Ephemeral protein binding to DNA shapes stable nuclear bodies and chromatin domains," *Biophys. J.*, vol. 112, no. 6, pp. 1085–1093, 2017.

[12] J. W. Cahn and J. E. Hilliard, "Free energy of a nonuniform system. I. Interfacial free energy, *J. Chem. Phys.*, vol. 28, no. 2, pp. 258–267, 1958.

[13] M. E. Cates and E. Tjhung, "Theories of binary fluid mixtures: From phase-separation kinetics to active emulsions," *J. Fluid Mech.*, vol. 836, p. 1, Feb. 2018.

[14] H. Y. Chan and V. Lubchenko, "A mechanism for reversible mesoscopic aggregation in liquid solutions," *Nat. Commun.*, vol. 10, no. 1, no. 2381, 2019.

[15] B. L. Clarke, "Stability of complex reaction networks," in *Advances in Chemical Physics*, I. Prigogine and S. A. Rice, Eds. New York, NY, USA: Wiley, 1980.

[16] M. C. Cross and P. C. Hohenberg, "Pattern formation outside of equilibrium," *Rev. Mod. Phys.*, vol. 65, p. 851, Jul. 1993.

[17] G. Giordano, C. C. Samaniego, E. Franco, and F. Blanchini, "Computing the structural influence matrix for biological systems," *J. Math. Biol.*, vol. 72, no. 7, pp. 1927–1958, 2016.

[18] P. C. Hohenberg and B. I. Halperin, "Theory of dynamic critical phenomena," *Rev. Mod. Phys.*, vol. 49, no. 3, pp. 435–479, 1977.

[19] Y. Hori, H. Miyazako, S. Kumagai, and S. Hara, "Coordinated spatial pattern formation in biomolecular communication networks," *IEEE Trans. Mol. Biol. Multi-Scale Commun.*, vol. 1, no. 2, pp. 111–121, Jun. 2015.

[20] Y. Hori and H. Miyazako, "Analysing diffusion and flow-driven instability using semidefinite programming," *J. R. Soc. Interface*, vol. 16, no. 150, Jan. 2019, Art. no. 1620180586.

[21] K. Kashima, T. Ogawa, and T. Sakurai, "Selective pattern formation control: Spatial spectrum consensus and Turing instability approach," *Automatica*, vol. 56, pp. 25–35, Jun. 2015.

[22] A. Klosin et al., "Phase separation provides a mechanism to reduce noise in cells," *Science*, vol. 367, no. 6476, pp. 464–468, 2020.

[23] Y. I. Li and M. E. Cates, "Non-equilibrium phase separation with reactions: A canonical model and its behaviour," *J. Stat. Mech. Theory Exp.*, vol. 2020, no. 5, May 2020, Art. no. 53206.

[24] F. A. Miranda-Villatoro and R. Sepulchre, "Differential dissipativity analysis of reaction-diffusion systems," *Syst. Control Lett.*, vol. 148, Feb. 2021, Art. no. 104858.

[25] J. D. Murray, *Mathematical Biology II: Spatial Models and Biomedical Applications*. New York, NY, USA: Springer, 2003.

[26] D. Osmanović and Y. Rabin, "Chemically active nanodroplets in a multi-component fluid," *Soft Matter*, vol. 15, no. 29, pp. 5965–5972, 2019.

[27] D. Osmanović and E. Franco, "Chemical reaction motifs driving non-equilibrium behaviors in phase separating materials," 2022, *arXiv:2207.10135*.

[28] A. van der Schaft, S. Rao, and B. Jayawardhana, "On the mathematical structure of balanced chemical reaction networks governed by mass action kinetics," *SIAM J. Appl. Math.*, vol. 73, no. 2, pp. 953–973, 2013.

[29] K. Shrinivas and M. P. Brenner, "Phase separation in fluids with many interacting components," *Proc. Nat. Acad. Sci. USA*, vol. 118, no. 45, Nov. 2021, Art. no. e2108551118.

[30] C. A. Weber, D. Zwicker, F. Jülicher, and C. F. Lee, "Physics of active emulsions," *Rep. Progr. Phys.*, vol. 82, no. 6, 2019, Art. no. 64601.

[31] D. Zwicker et al., "Growth and division of active droplets provides a model for protocells," *Nat. Phys.*, vol. 13, pp. 408–413, Apr. 2017.

Open Access funding provided by 'Università degli Studi di Trento' within the CRUI CARE Agreement